Effect of Scan Rate and pH on Determination Amoxilline Using Screen Printed Carbon Electrode Modified with Functionalized Graphene Oxide

Issam A.Latif
Sundus H. Merza
Dept. of Chemistry/ College of Education for Pure Science (Ibn Al-Haitham) /University of Baghdad
issom400@gmail.com
Received in:17/August/2017, Accepted in:1/November/2017

Abstract

Graphene oxide GO was functionalized with 4-amino, 3-substituted 1H, 1, 2, 4 Triazole 5(4H) thion (ASTT) to obtain GOT. GOT characterized by FT-IR, XRD.via modification of the working electrode of the SPCE with the prepared nanomaterial (GOT) the effect of scan rate and pH on the determination of Amoxilline (AMOX) was studied using cyclic voltammetry. AMOX show various responses at pH ranging from 2 to 7 and also was observed sharp increase in the oxidation peaks in the pH 3. The formal potential (midpoint) for AMOX was highly pH-dependent. From the effect of scan rate, surface coverage concentration Γ of electroactive species the values of the electron transfer coefficient and the electron transfer constant rate k_{et} was obtained as 5.39×10^{-10} molcm^{-2}, 0.5, and 2.45×10^{-3} cm.s^{-1}respectively.

Keyword: screen printed carbon electrode, cyclic voltammetry, Thiocarbohydrazide, Graphene oxide,Amoxilline.

Introduction

Graphene oxide is one layer of a polycyclic hydrocarbon network and is partially aromatic, has various oxygen functional groups (CO, OH, and COOH) prepared from the oxidative treatment of bulk graphite (Hummer method) [1] [2].Presence of high density electronegative oxygen atoms on the GO basal plane, gives rise to an energy gap in the electron density of states [3] making GO non-conductive.The hydroxyl and the epoxide groups lay on the surface sheet while carbonyl and carboxyl groups attached at the edge. Carboxylic groups were used to react with thiocarohydrizde (TCH) by cyclocondensation reaction. This could be allowed to prepare GO-4-amino,3-substituted 1H,1,2,4 Triazole 5(4H) thion(ASTT) (GOT)
Individual layers of GO can be obtained by sonication and by stirring aqueous suspension for long enough [4]. Electrochemical sensor based Graphene oxide was often used to determin various drugs and biological molecules such as dihydronicotinamide adenine dinucleotide (NADH)[5]and diethylstilbestrol(DES)[6]. This work is concerned with study of voltammetric behavior of Amoxicillin (AMOX) at screen printed carbon electrode modified withGraphene oxide functionalized at the edge of sheet and studies their impact to determine Amoxilline(AMOX).
Amoxicillin (2S, 5R, 6R)-6{[(2R)-2-amino-2-(4-hydroxylphenyl)-acetyl] amino}-3, 3-dimethyl-7-oxo-4-thia-1-azabicyclo [3.2.0] heptane-2-carboxylic acid, belongs to a class of antibiotic, called the Penicillin contains a β-lactam ring figure (1) which is responsible for its anti-bacterial against Gram-positive and Gram-negative bacteria.

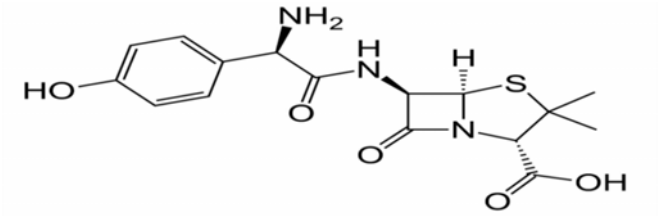

Figure (1): Structure of Amoxilline

Experimental

Chemicals and reagents

AMOX antibiotic from Samarra drugs factory was used without further purification .The phosphine buffer solution PBS was made up by mixing solutions of sodium phosphate dibasic Na_2HPO_4 and sodium phosphate monobasic dihydrate$NaH_2PO_4.2H_2O$ from Fluke, adjusted by 1M H_3PO_4 or 1M NaOH (MERCK). Tri distilled water was used for all preparations.

Apparatus

Electrochemical measurement was recorded on a portable potentiostatμ Stat 200 (Drop Sens S.L. Oviedo, Spain).The principle function of a potentiostatis controlling potential and measuring current; which was connected via a USB connection to laptop computer installed with the measurement software Drop View (DropSens DRP-110). The measurement was made with screen printed carbon electrode (SPCE) having, carbon counter electrode CE, silver/silver chloride reference electrode RE and a carbon working electrode WE (4 mm diameter) printed on a ceramic surface[8],a small area enables very small sample to perfome the measurement. Volumes smaller than 10 µl deposited directly on the electrode surface [9] are adequate for the analysis. All of the pH measurements were made with a PH-meter BP3001. Functionalized GO was dispersed with an ultrasonic instrument type (soniprep 150).Powder

XRD analysis was carried out by using powder diffractometer (Japan) XRD Shimadzu 6000 with an incident Cu-Kα radiation of 1.54A° 40.0Kv and 30mA; scan range (2θ= 5-80°) and; scan speed: 10 (deg/min).). FTIR spectra were obtained on Shimadzu IR affinity 8400s, Japan. Scan range 4000–400 cm^{-1} with a resolution of 4 cm^{-1}.Infrared spectrophotometer using potassium bromide disc.

Preparation of Graphene oxide

Graphite oxide (GTO) was synthesized by hummers' method [2]. The GTO mixture formed was filtered and washed with 5% aqueous solution HCL and distilled water until the pH of the rinsing water became (6-7). The product was dried at 55 c° for 48h. The Graphite oxide GTO aqueous solution mixture was exfoliated by sonication and stirring for 25 min [4] to obtain aqueous colloidal of Graphene oxide GO sheet.

Preparation of Thiocarbohydrazide

Thiocarbohydrazide TCH was prepared [10] by reaction of hydrazine N_2H_4 with carbon disulfide CS_2 at 10 $c^{\circ}$with stirring until formation of yellow precipitate to produce hydrazinium dithiocarbazinate HDTC as in equation 1.

$$CS_2 + 2N_2H_2 \rightarrow H_2NHNCS_2H.N_2H_4 \qquad (1)$$

The resultant mixture refluxed for half hour to remove hydrogen sulfide H_2S as in equation 2.

$$H_2NHNCS_2H.N_2H_4 \rightarrow H_2N-NH-CS-NH-NH_2 \qquad (2)$$

The reaction mixture was filtrated to separate the crystalline precipitate of TCH then washed with ethanol and water. The TCH crystals were dried with vacuum oven for 6 hours at 40-50 c°.

Functionalization of GO with TCH

Carboxylic groups in GO can be used as starting point to react with TCH at its melting temperature in cyclocondensation reaction. This could be allowed to prepare GO-4-amino,3-substituted 1H,1,2,4 Triazole 5(4H) thion(ASTT),(GOT) as shown in Fig. (2).The product GOT was cooled, washed with distilled water to dissolve the non-reacted TCH and dried at 60c°.

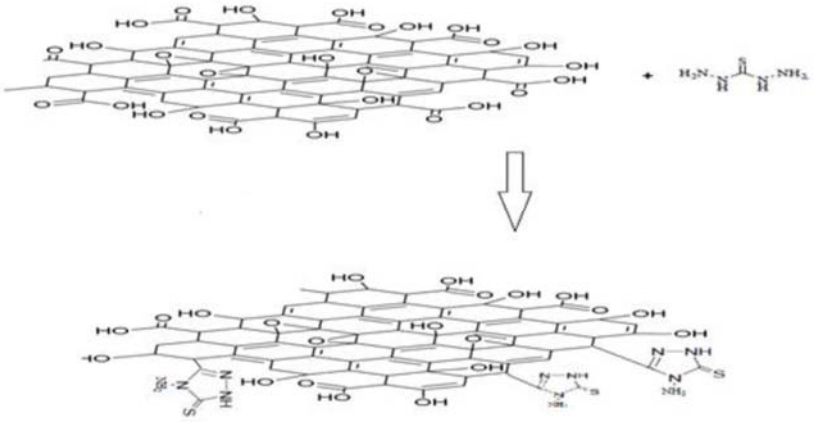

Figure: (2) Functionalize Graphene Oxide GO with TCH.

Fabrication of the modified electrode

1 mg of purified GOT andGO was dispersed into 10 ml of redistilled water and 3µL Nafion and for 1 h sonicated. The modified electrode was made by coating the WEby dropping of 4 µL from the above mixture. Then 50µL from freshly prepared solution of AMOX was dropped on reservoir area to cover modified working electrode, counter and reference electrodes for at least one minute.

Pretreatment of SPCEs

At scan rate 0.1 V s^{-1} the potential was swept between −0.5 and +1.0 V in 0.1 M H_2SO_4 in order to pretreat the SPCE and to get a reproducible voltammogram increase sensitivity of sensors as well as to obtain a stable baseline for long term experiments [11]. Then, the SPCE was washed with double distilled water and dried at room temperature 24-25℃.

Results and discussion

Characterization of modifiers GO and GOT

FT-IR of thiocarohydrizde (TCH)

Figure (3) shows FT-IR spectrum of prepared TCH. The peaks at 3273.2, 3209.5, 3305.9 cm^{-1}corsspondes to N-H and NH_2 stretching vibrations respectively. The NH2 bending and wagging vibrations contributed to the two peaks at 1643.35 and 1143.79 cm-1 respectively [12]. The characteristic peaks 1531 and1500.6 cm-1 assigns to the coupled modes N-H wagging and C-N stretching vibrations [13].The C=S stretching contributes to two peaks at 1288 cm-1 and 935 cm-1 also these peaks contain contributions of other vibration such as C-N stretching and C-N-N bending vibration .

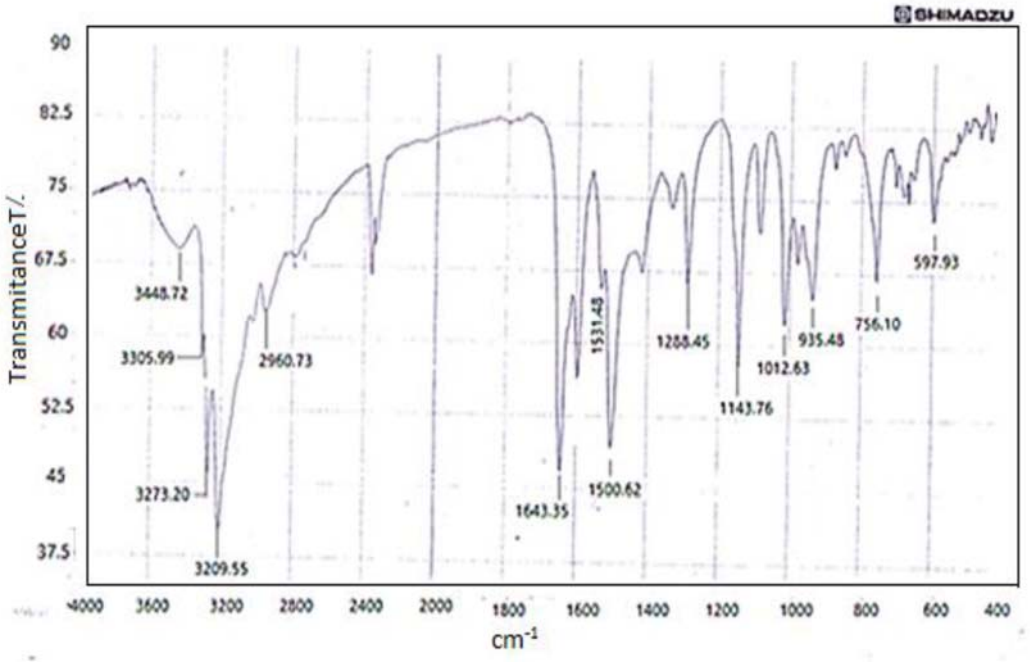

Figure:(3) FT-IR spectrum of TCH

FT-IR of GO

Fig. (4) Shows the FT-IR spectrum of GO. The stretching vibration of (C-OH, COOH, and residue of H2O) appeared at 3401 cm^{-1} with broad and strong band. The peak at 1587cm^{-1} was assigned to unoxidized graphitic domain.

The two bands at 1221 cm^{-1} and 1400 cm^{-1} were corresponded to (C-O) stretching vibration of epoxide groups (C-O-C) and (C-O-H) bending vibration of COOH group or C-OH group respectively. The OH bending vibration of COOH groups can be used to evaluate the amount of COOH groups [14]. Vibration at 1060 cm^{-1} is assigned to alkoxy (C-OH) groups. Besides, the band at 1721 cm^{-1} might refer to not only the carbonyl group stretching vibration of COOH situated at the edges but also to ketones or quinone [15].

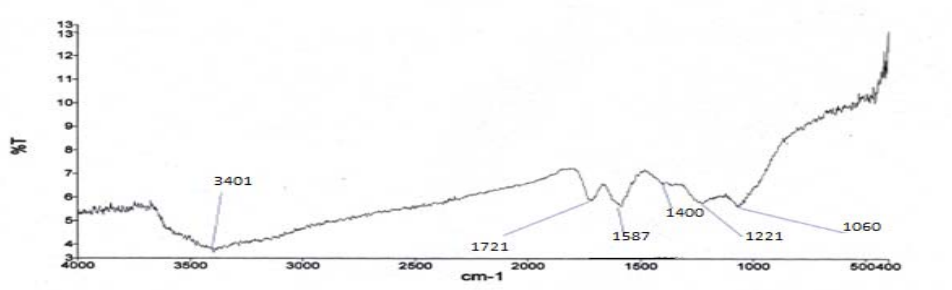

Figure:(4) FT-IR spectrum of GO

FT-IR of functionalize GO with TCH

The infrared spectrum of GO functionalized with Thiocarbohydrazide (GOT) shown in figure (5) the peaks in the region 3000-3500 referred to stretching vibration of NH2 groups. These peaks were not appeared in the FT-IR spectra of GO and they were suggested to the formation of functionalization of GO with TCH.A band in the 1590-1650 cm^{-1} region is characteristic of the NH2 scissoring vibration; additionally, absorption band at 750-850cm^{-1} assigns to NH2 twisting and wagging deformations. Also , absorption bands at 1333.32, 1501.4, 1175cm^{-1} that appeared in spectrum of (GOT) correspond to stretching vibration of (C=S) , C=N, and N-N respectively which denotes to stretching vibration that had been introduced to GO by functionalized with TCH.

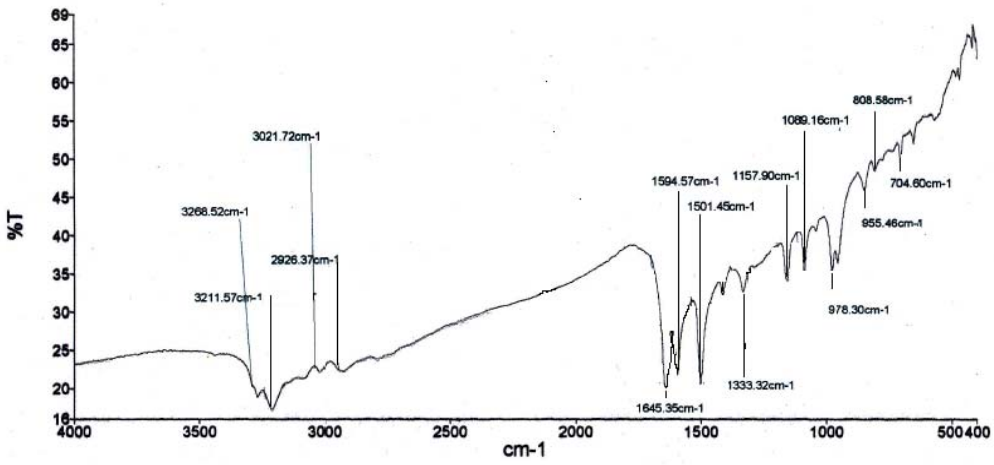

Figure :(5) FT-IR spectrum of GO functionalized with TCH

XRD

XRD of GOA powder sample of GO was examined with x-rays diffract meter. Figure (6) shows the XRD pattern of GO. It is found that GO exhibits a strong diffraction at 11.95° corresponding to d-spacing of 0.73 nm [16, 17] which is higher than that of graphite (0.336 nm) indicates introduced functional groups (carboxylic acid, carbonyl, hydroxyl and epoxy) on the basal and edges planes of GO sheets [18] Moreover, the increase in d-spacing proved the oxidation of graphite flakes (GT) Since the degree of oxidation is proportional to the interlayer spacing (d) of GO [19].

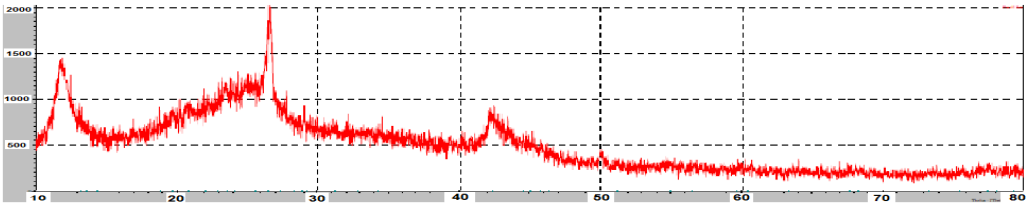

Figure: (6) XRD patterns of GO

Surface area study

The effective area of the electrodes a bare SPCE ,GO-SPCE and GOT-SPCE was calculated in a solution of 0.5mM $3[Fe(CN)_6]^{-3}$ in 0.1M KCl, using Randles Sevick equation [20] at different scan rates ranging from 0.01 to 0.1V.s^{-1}

$$I_p=2.69\times10^5 A n^{3/2} D R^{1/2} c v^{1/2} \qquad (3)$$

Where (Ip) refers to the peak current, (A) is the surface area of electrode cm2, n is the number of electrons ,DR is diffusion coefficient, C is the concentration of K3 $[Fe(CN)_6]^{-3}$and υ refers to the scan rateVs-1.For Potassium ferricyanide , DR = 7.6×10^{-6} cm^2 s^{-1}[21],and n=1.The redox behavior of 0.5mM $K3[Fe(CN)_6]^{-3}$ in 0.1M KCl was investigated by cyclic voltammetry. The redox peak currents at bare SPCE, GO-SPCE and GOT-SPCE increased linearly with scan rate ranging from 0.01 to 0.1V. s^{-1} as shown in figures (7), (8) and (9) respectively. The apparent electroactive area values was found for the electrodes bare SPCE, modified electrode GO-SPCE and GOT-SPCE to be 0.04 cm^2, 0.05 cm^2 and 0.06 cm^2 respectively. This enlargement in the effective surface area proved the modification of bare SPCE with GO and GOT.

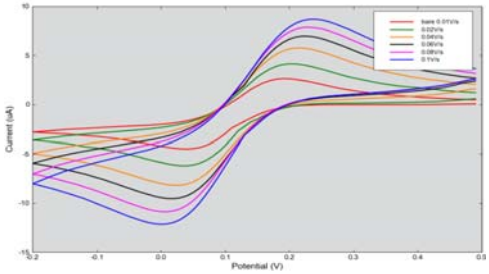

Figure (7): Cyclic voltammogram for bare/SPCE in ferricyanide

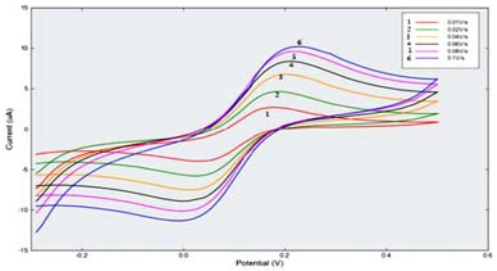

Figure (8): Cyclic voltammogram for GO-SPCE in potassium ferricyanide potassium

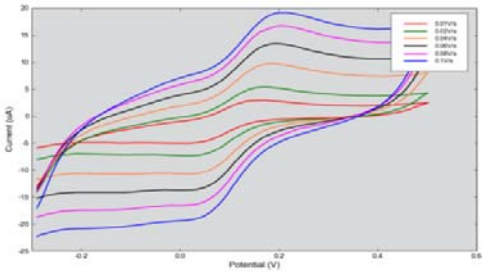

Figure: (9) Cyclic voltammogram forGOT-SPCE in potassium ferricyanide

Effect of pH

The influence of pH on the oxidation peak current and potential of 0.5mM AMOX in PBS pH range from2 to 8 at the GOT-Nafion modified SPCE was investigated by CV at scan rate 0.1V.s^{-1}. AMOX shows significant response figure (10). The redox peaks current varied with pH values. The redox peak at pH3 was appeared with higher oxidation and reduction current values.

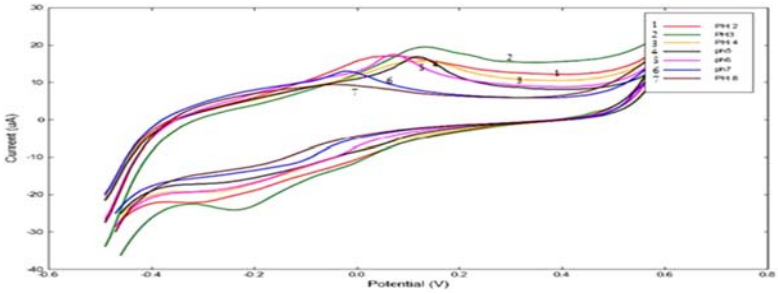

Figure: (10) Cyclic voltammogram obtained at GOT-Nafion/ SPCE with 0.5mM AMOX in PBS with different pH values at scan rate 0.1v.s^{-1}.

There was no response of blank PBS in GOT-Nafion/ SPCE in all pH range indicated that the current and potential value of the oxidation and reduction were due to the AMOX only.
The anodic peak current values of AMOX at the GOT-SPCE were plotted versus pH values of the supporting electrolyte (PBS). Figure (11) reveals that the sharp increase in the oxidation peaks in the pH range of 2-3 this may be due to fast electron process then decreased in the range of 3 to 4 this can be related to change of AMOX interaction with surface of modified SPCE (GOT) [22]. Gradually increase in current was observed as the pH values increased from 4 to 6 due to oxidation ability of AMOX, where the electrochemical response of AMOX in pH7 was low. Considering all these points, the pH3 was with highest current value and show clear redox peak than the other pH values.

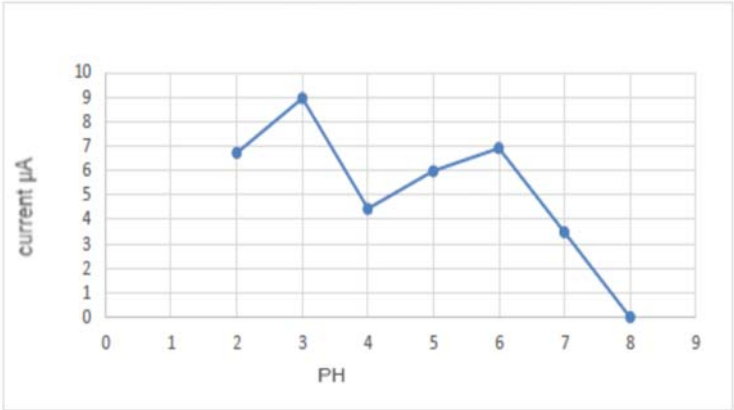

Figure: (11) Plots of peak current I_p for oxidation 0.5mM AMOX at GOT-Nafion / SPCE *vs*pH of electrolyte solution PBS (pH3) in 0.1KCl

Cyclic voltammetry CV is a powerful tool for identifying and studying proton and electron transfer (PET). If a process involving m-protons and n-electrons as shown in equation.

$A+mH+ne\rightleftharpoons$ (4)

For Nernst equation, assumption the electrode process was electrochemically reversible, we can write [23].

$E=E_{f^\circ}(A/B)-RT/nFln$ [B]/[A]$[H+]^m$ (5)

$E=E_{f^\circ}(A/B)+RT/nFln[H+]^m-RT/nFln[B]/[A]$ (6)

$E=E_{f^\circ}(A/B)-2.303mRT/nFpH-RTnF/[B][A]$ (7)

For a chemically reversible half reaction, the pH dependence of a PET couple is given by eq (8)[23].

$E_{f,^\circ}=E_{f^\circ}(A/B)-2.303mRTnF/pH$ (8)

$E_{f,^\circ}$ was an effective formal potential, the potential midway between the peaks for redox peaks for A and B. The dependence formal redox potential E° of AMOX on the pH was investigated by cyclic voltammetry. The E° value was obtained from the average value of anodic potential and cathodic potential. Fig. (12) shows that the formal potential (midpoint) of AMOX was highly pH-dependent. However, It was found that the E° values shifted to more negative values (decrease linearly) with increase in pH buffer solution. Between pH 2 and 3, a slope has value agreement with the theoretical value of 0.06V [24, 25] according to the equation.

$E^\circ=-0.065pH+0.26$ (9)

These results of the electrochemical oxidation of Amoxicillin cconfirm the involving of equal number of electrons and protons [26] then the potential returned to be shifted to more positive values between pH 3-7 with a slope 0.0315 V/pH according to the equations.

$E^\circ=0.0315pH-0.0375$ (10)

This behavior may be due to the involving of two electrons and one proton in electrochemical oxidation process of AMOX in this pH range [27]. The intersection of the curve was located at pH 3 corresponding to the apparently pKa. The value of pKa is in agreement with A.T.suji et al[28] and GN. Rolinson[29]

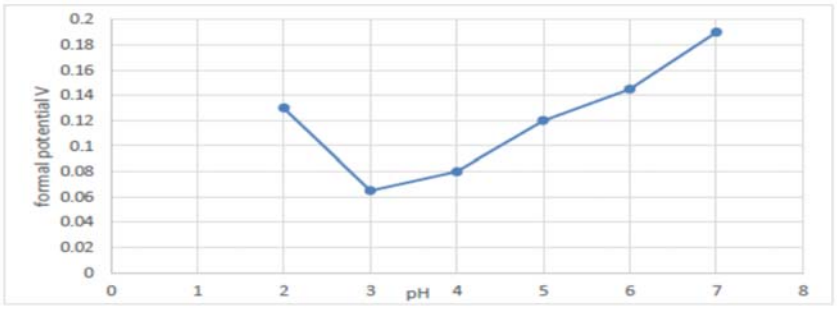

Figure: (12) Plots of formal potential E° for oxidation 0.5mM AMOX at GOT-Nafion/ SPCE *vs*pH of electrolyte solution PBS ranging from (pH2-pH7) in 0.1KCl.

The cyclic voltammograms for bare SPCE, GO-SPCE and GOT-Nafion/SPCE in 0.1M blank phosphate buffer solution (pH 3.0) and in the presence of 0.5 mM AMOX is shown in figure (13). The potential was swept from - 0.5V to 0.6V at scan rate 0.1V.s^{-1}. When the SPCE coated with GO (5 curve) redox peaks for AMOX were observed at 0.12 V with anodic peak current (13.186µA) and at -0.05V with cathodic peak current (15.904µA). The cyclic voltammogram of GOT-Nafion/SPCE in blank 0.1 M phosphate buffer solution (pH 3.0) showed broad anodic and cathodic peaks (4curves). But in the presence AMOX (3 curves), the anodic peak current was appeared at about 0.08 V (anodic current16.443µA), with cathodic peak on the reverse scan at -0.3V (cathodic current 17.393µA). The increase in redox signal may be attributed to the functionalization of GO with 4-amino-3mercapto1, 2, 4-triazol at the edge of GO sheet which facilitate the electron movement between AMOX and the electrode surface and also could be attributed to GOT which has higher effective surface area. Based on this, GOT-Nafion/SPCE can be used as electrochemical sensing for sensitive determination of AMOX. At the bare SPCE in presence AMOX (1 curve) no redox peak can be seen indicating oxidation process of AMOX hard to occur due to surface of SPCE has small amounts of oxygenated functionalities [30]. On the other hand, the bare SPCE have no electrochemical response in blank PBS (2 curve).

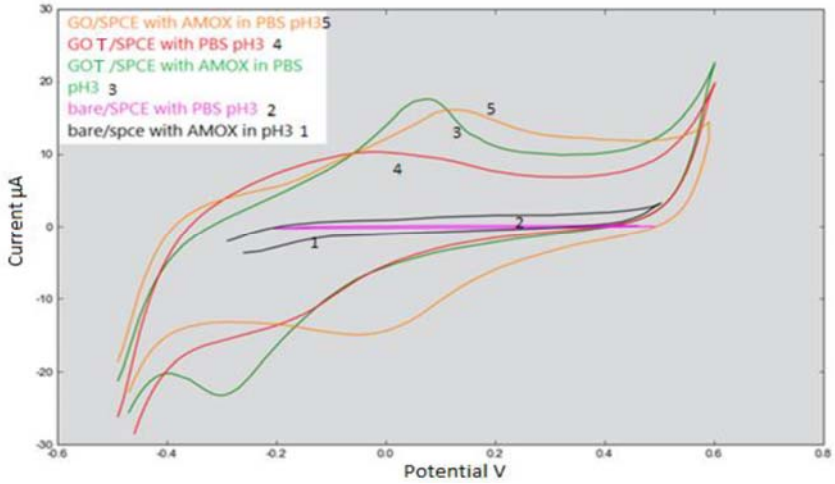

Figure: (13) Cyclic voltammogram of 0.5mM AMOX in 0.1M PBS (pH 3.0) at scan rate 0.1v.s-1at bare and GO-T-Nafion/SPCE.

Effect of scan rate

The effect of the potential scan rate on the electrochemical process was studied to understand the electrode behavior and the reversibility of electrode reactions. Cyclic voltammogram of GOT-Nafion/SPCE in the supporting electrolyte solution PBS (pH3) containing 0.5 mM AMOX at different scan rates from 0.01 to 0.1V. s^{-1} which are shown in figure (14).

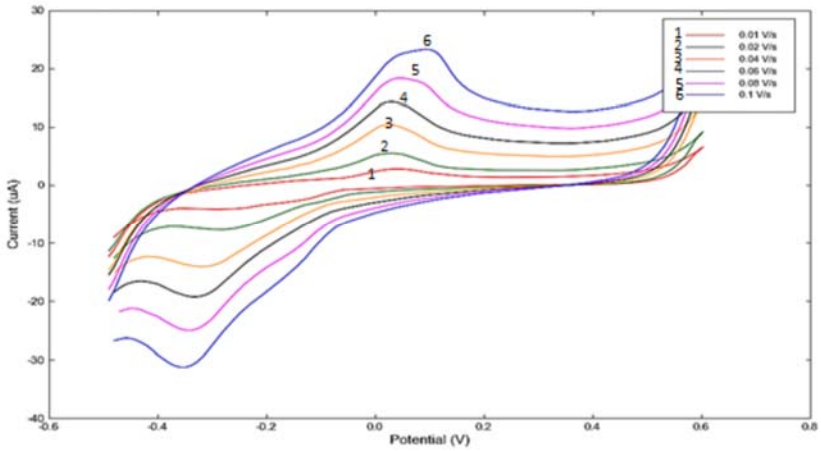

Figure :(14) Cyclic voltammogram of 0.5mM AMOX in pH3 PBS obtained with various scan rates (0.01-0.1 V.s^{-1}).

With increasing the scan rate, the oxidation and reduction peak current represent good linear relationship with the scan rates, correlation coefficient 0.9921 and 0.9976 respectively figure (15)

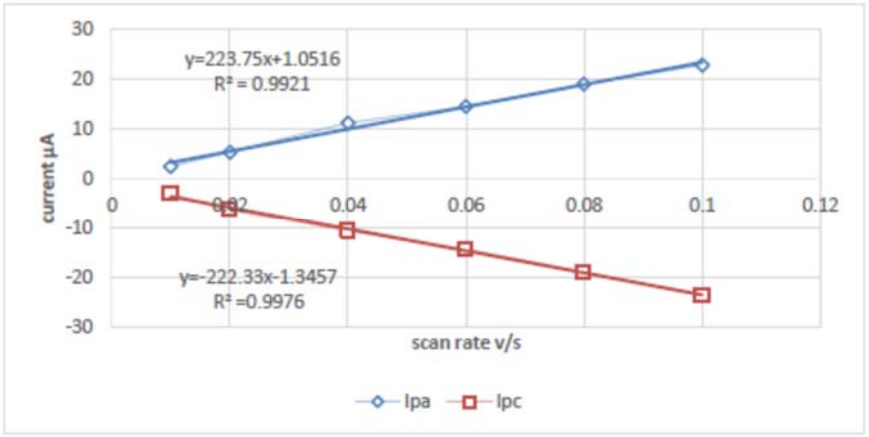

Figure: (15) Variation of the peak current (I_{pa}) and (I_{pc}) with the scan rate for 0.5 mM AMOX.

The peak current is proportional to, scan rate υ, surface coverage concentration Γ of electroactive species and number of electrons n according to the following equation [31]

$I_{Pa} = n^2F^2\,\Gamma A\upsilon/4RT$ (11)

A is the surface area (cm^2). The electroactive coverage must be high enough for a current to be observed. the surface coverage concentration of 0.1mM (AMOX) at the surface of GOT-SPCE can be estimated to be about 5.39×10^{-10}mol cm^{-2} (n=2) or 3.246×10^{14} molecules.cm^{-2}.

At scan rates between 0.01 and 0.1 $V.s^{-1}$ .the peak heights of the anodic and the cathodic signals were proportional to scan rate and the ratio was almost equal. The difference of the peak potentials is significantly bigger than 59 mV and the separation of the two signals is constant at 0.35 V ± 3 V. Therefore, the redox reaction of AMOX can be considered to be reversible this means the electrode practically remain in equilibrium with an oxidized form of AMOX as shown in table (1) [33].

Table:(1) Peak to peak separation and peaks current ratio for AMOX at different scan rate obtained from figure (17)

Scan rate ($V.s^{-1}$)	E_{pa}-E_{pc} (V)	I_{pa}/I_{pc}
0.01	0.33	1.06
0.02	0.32	0.85
0.04	0.35	1.05
0.06	0.36	1.01
0.08	0.38	1.005
0.1	0.38	0.96

In addition, the relationship between I_{pa}, I_{pc} and $\nu^{1/2}$ was studied figure (16). The redox peaks current were proportional to the square root of scan rate which proposed the process was a diffusion-controlled in solution [32] when transport the redox species of AMOX in solution to and from electrode.

The slope of the curve for the two processes, almost the same which means the redox process occurs with the same electron transfer rate[34].

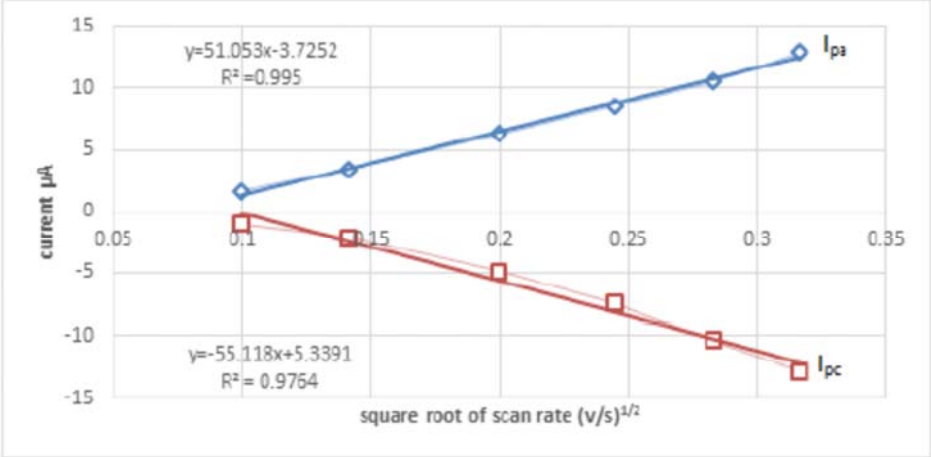

Figure: (16) Relationship between I_{pa} and I_{pc} vs.square root of scan rate for GOT modified SPCE.

The diffusion and adsorption of electrode process were studied and a plot of a logarithm of peaks current *vs.* logarithm of the scan rate gave a straight line with a slope of 0.9494 for foreword scan and 0.8597for reverse scan is shown in figure (17). This value is close to that found in the literature [35]. The slope of the straight lines was intermediate value between 1 the theoretical value of the adsorption controlled electrode process and the theoretical value of 0.5 which was expressed for the diffusion controlled electrode process, this indicated that the electrode process was controlled simultaneously both by diffusion and adsorption [36] for oxidation and reduction process.

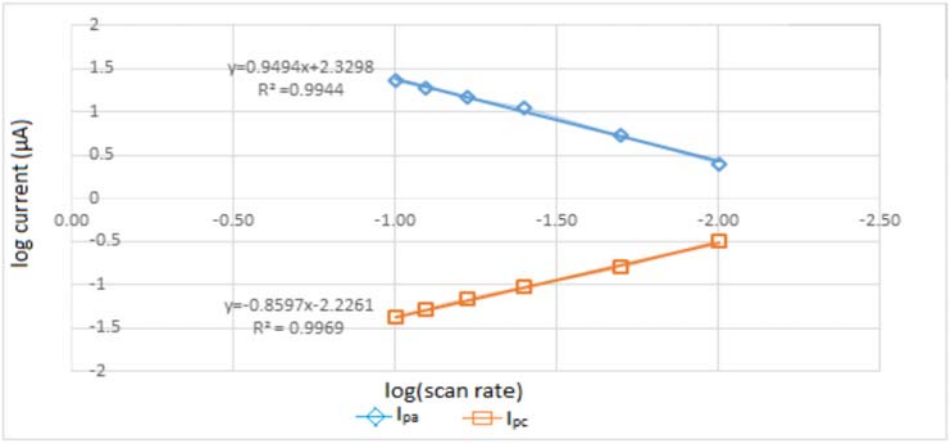

Figure: (17) Log current vs. log υ for GOT modified SPCE in presence AMOX.

The models developed by Laviron were developed to provide a quick estimate of the electron transfer rate constant κ using cyclic voltammetry. This method count on the electron transfer coefficient (α) (dimensionless parameter), which was a measure of the symmetry of the energy barrier of the redox reaction. To determine α, the peak potential Epis plotted vsln scan rate ν [37, 38]. The peak potentials can be described by following equations.

$E_{pa}=E^{\circ}+(1-\alpha)nF\ln\upsilon$ (12)

$E_{pc}=E^{\circ}+R$ (13)

E° is formal potential, R is the gas constant, n is the number of electrons involved in the redox reaction, T is the absolute temperature in Kelvin, F is the Faraday constant, and υ is the scan rate. The cathodic peak potential (E_{pc}) is changed linearly as the function of scan rate in range from 0.01 to 0.1V.s^{-1}. A linear regression equation is shown below.

$E_{pc}=-0.0277\ln\upsilon+0.4096$ (14)

From the slope of Fig. (18) and taking the electron transfer coefficient 0.5 according to R.Guidelli*et al* [39] the number of electrons was estimated to be (n~2) this value is in agreement with value obtained from pH measurement. The E_{pa} effort non-linear relationship .The electron transfer rate constant k_{et} was obtained by introducing the values α, a scan rate 0.1V.s^{-1}, and ΔE_p = 0.38V in the following equation [40].

$lnks=(1-\alpha)+(1-\alpha)ln\alpha-lnRT/nF\upsilon-\alpha(1-\alpha)nF\Delta E/RT$ (15)

The heterogeneous electron transfer rate constant is 2.45×10^{-3} cm.s^{-1}. This value indicates a slow kinetics and longer time requirement for equilibrium [37]

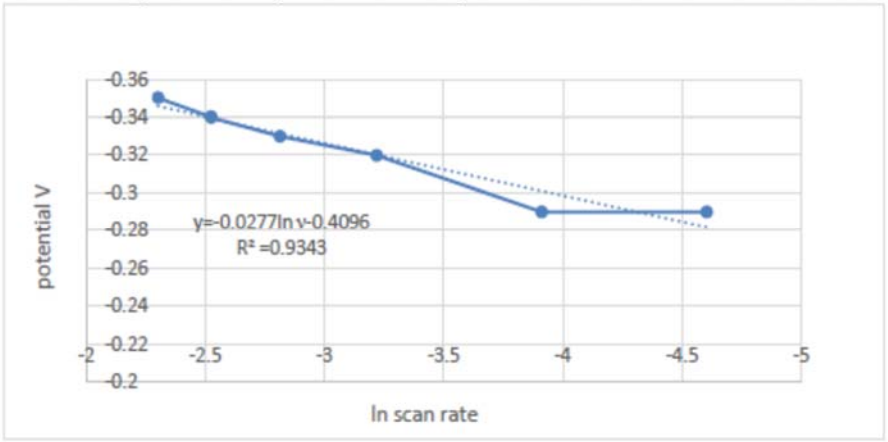

Figure (18): Potential versus natural logarithm of scan rate for GOT-SPCE /AMOX.

4. Conclusion

The voltammetric studying shows the peak current arises not only of AMOX molecules which were already adsorbed on the GOT-SPCE surface but also of those which reach to the electrode by means of diffusion. These results reveal that the anodic process was dominated by partially adsorption (adsorbed AMOX at the electrode) and partially diffusion of AMOX through the diffusion layer simultaneously, that may be changed with the changing of the modifying materials, and also the heterogeneous electron transfer rate constant was2.45×10^{-3} $cm.s^{-1}$. This value indicated a slow kinetics and longer time requirement for equilibrium and depending also on the modifying materials (GOT).

The modifying materials play a very important role in the kinetic of the electrochemical reaction on the SPCE.

5. References

[1] C. Marcano ; V. Daniela kosynkin.Dmitry, , berlin Jacob M . Alexande, S. r7 and Zhengzong S. Improve synthesis of Graphene oxide ACS NANO 4(8); 4806-14. 2010.

[2] W.S. Hummers and R.E. Offeman Preparation of Graphitic Oxide. Journal of the American Chemical Society, 80(6): p. 1339-133. 1958.

[3] I .Jung, Tunable Electrical Conductivity of Individual Graphene Oxide sheets reduced at Low Temperatures. Nano Letters, 8(12): p. 4283-4287. 2008

[4] I. Jung, simple approach for high –contrast optical imaging and characterization o fgraphene based sheets. Nano Lett.7, 3569-3575. 2007.

[5] L. Zhang;Li YZhan,L. g We,D. Li i. Karpuzov,D., Tao long Y. Electrocatalytic Oxidation of NADH on Graphene oxide and reduced Graphene oxide modified screen printed electrode Int.J.Electrochem.sci,6819-829. 2011

[6] Ch.Yu;W .Ji; Y.Wang ;N. Bao and H.GuGraphene Oxide –modified electrods for sensitive determination of Diethylstilbesrtol .Nanotechnology 24115502, 2013.

[7] M. Akhond,; G. Absalan, and Ershadifar, H,Highly sensitive colorimetric determination of amoxicillin in pharmaceutical formulations based on induced aggregation of gold nanoparticles. Spectrochim. Acta Part A Mol. Biomol. Spectrosc., 143, 223–229, 2015.

[8] M.F. Bergamini and M.V.B. Zanoni, Anodic Stripping Voltammetric Determination of Aurothiomalate in Urine Using a Screen-Printed Carbon Electrode: *Electroanalysis18,*1457, 2006.

[9] Lucarelli;F. Authier; L., Bagni; G. G., Baussant T.; Aas, E. and Mascini. M. DNA Biosensors Investigations in Fish Bile for Use as a Biomonitoring Tool, Analytical Letters, 36, pp. 188(2003).

[10] Sun XH. and Liu Y Burn F, study on the synthesis of thiocarbohydrazide chemistry (china) 621999:46-48. 1999.

[11] Vasilescu A., Andreescu S., Bala C., Litescu S.C., Noguer T. and Marty J.L. (2003) Screen printed electrodes with electropolymerizedMeldola Blue as versatile detectors in biosensors, Biosensors and Bioelectronics 18 781–790.

[12] Burn G.R. (1968). Metal complexes of thiocarbohydrazide .Inorg.chem.7 277-283.

[13] Shao G., Yonggen Lu, Fangfang W., Yang Ch., Zeng F. and Wu Q.,. Graphene oxide: the mechanisms of oxidation and exfoliation. J. Mater. Sci .47(2012)4400–4409.

[14] D.Yang, A. Velamakanni, G. Bozoklu, S. Park,M. Stoller, R.D.Piner, S. Stankovich,I. Jung, D.A. Field, C.A.JrVentrice and R.S. Ruoff . Chemical analysis of GO films after heat

and chemical treatment by X-Rays photoelectrons and micro- Raman spectroscopy .Carbon 47 (2009)145.

[15] A. Shalaby; D. Nihtianova; P. Markov; A. D. Staneva;R. S. Iordanova and Y. B. Dimitriev. Structural analysis of reduced graphene oxide by transmission electron microscopy. Bulgarian Chemical Communications, 47(1): 291–295. 2015

[16] H. Yang; J. Jiang;W.Zhou; L. Lai; L.Xi; Y.Ming Lam; Z. Shen; B. Khezri and T. Yu. Influences of graphene oxide support on the electrochemical performances of graphene oxide-MnO2 nanocomposites. Nanoscale Research Letters, 6(2011)531. 176

[17] Y.Zhang;T.T. Tang; C. Girit;Z. Hao; M.C. Martin;A. Zettl, M.F. Crommie, Y.R. Shen and F.Wang. Direct observation of a widely tunable bandgap in bilayer graphene. Nature, 459(7248): 820-823. 2009)

[18] D. C. Marcano,; Kosynkin, D. V. Berlin, J. M. Sinitskii, A. Sun, Z. Slesarev, A. Alemany, L. B. Lu and J.M. Tour. Improved synthesis of graphene oxide. Acs Nano, 4(8): 4806. 2010

[19] Chen, L. Xu; Z. Li, J. Min, C. Liu, L. Song, X. Chen, G. and X. Meng. Reduction and disorder in graphene oxide induced by electron-beam irradiation. Materials Letters, 65(8): (2011) 1229-1230.

[20] A.J. Bard and L.R. Faulkner. Electrochemical Methods: Fundamentals and Applications. Second ed. Wiley, New York, 2001.

[21] S. Y. Grewal; J. A. Muhammad Shiddiky, A. G.Sean,K. M. Weigel,G. A.Cangelosi, and M. Trau. Label -free electrochemical detection of an Entamoebahistolytica antigen using cell -free yeast-scFv probes. The Royal Society of Chemistry ,2013

[22] A. R. Fakhari; A. Sahragard and H. Ahmar. Development of an electrochemical sensor based on reduced graphene oxide modified screen-printed carbon electrode for the determination of buprenorphine. Electroanalysis 26 (11): (2014)2474–2483.

[23] R.G. Compton and C.E. Banks, Understanding Voltammetry .World Scientific, Singapore, 2007.

[24] I. Martins; F.C. Cristiani; S.C. Larissa; A. Francisco, M.C. Leticia and R. Susanne. Determination of parabens in shampoo using highperformance liquid chromatography with amperometric detection on a boron-doped diamond electrode, Talanta 85 ,2011 1–7.

[25] A. Muhammad;N.A. Yusof ;R. Hajian , and J.Abdullah Construction of an electrochemical sensor based on carbon nanotubes/gold nanoparticles for trace determination of Amoxicillin in bovine milk. Sensors (Basel). 16(1) : 2016. 56.

[26] W. Sun; M. Xi; L.Zhang; T. Zhan; H. Gao and K. Jiao. Electrochemical behaviors of thymine on a new ionic liquid modified carbon electrode and its detection. Electrochim. Acta 56,2010,222–226.

[27] H. R. Zare; N. Nasirizadeh; M. Mazloum-Ardakani, and M. Namazian. Electrochemical properties and electrocatalytic activity of hematoxylin modified carbon paste electrode toward the oxidation of reduced nicotinamide adenine dinucleotide (NADH). Sensors and Actuators B: Chemical. 120(1): 288–294. 2006

[28] A.T. suji; E .Nakashima; S. Hamano and T.Tamana. Physiochemical properties of amphoteric β-lactam antibiotics, I: stability, solubility, and dissolution behavior of amino penicillins as a function of Ph. J Pharm Sci. 67(8): (1987)1059-66.

[29] G.N.Rolinson and AM. Geddes. The 50th anniversary of the discovery of 6-aminopenicillanic acid (6-APA).Inter J Antimicrobial Agent. 29 ,3–8. 2007

[30] S.C.Wang; K.S. Chang and C.J. Yuan. Enhancement of electrochemical properties of screen-printed carbon electrodes by oxygen plasma treatment. ElectrochimicaActa 54 4937–4943. 2009

[31] M. Sharp; M. Petersson and K. Edström . Preliminary determinations of electron transfer kinetics involving ferrocene covalently attached to a platinum surface J. Electroanal. Chem. Interfac. Electroch. 95 (1979) 123.

[32] H.V. Tran, B. Piro, S. Reisberg, H.T. Duc and M.C. Pham. Antibodies directed to RNA/DNA hybrids: an electrochemical immune sensor for microRNAs detection using graphene-composite electrodes. Anal. Chem. 85 ,8469–8474. 2013

[33] N. Tsierkezos and U. Ritter. Synthesis and electrochemistry of multi-walled carbon nanotube films directly attached on silica substrate. J. solid state electrochem.14 (2010)1101–1107.

[34] M.M. Barsan; E. M. Pinto and Ch. M.A. Brett. Electrosynthesis and electrochemical characterization of phenazine polymers for application in biosensors. ElectrochimicaActa 53 ,3973–3982. 2008

[35] F. Li, J. Song, D. Gao, Q. Zhang, D. Han and L. Niu. Simple and rapid voltammetric determination of morphine at electrochemically pretreated glassy carbon electrodes. J. pure and applied Anal. Chem. 79 ,845–850. (2009)

[36] K.David and J. Gosser. Cyclic voltammetry, simulation and Analysis of reaction mechanisms. VCH publishers, 42-43. 1994

[37] E.Laviron. General expression of the linear potential sweep Voltammogram in the case of diffusionless electrochemical systems. J. Electroanal. Chem. 101 ,19-28. 1979

[38] Q. He, T. Gan; D.-Y. Zheng and S.S. Hu. Direct electrochemistry and electrocatalysis of nitrite based on nano-alumina-modified electrode, Journal of Solid State Electrochemistry 14 ,1057. 2010

[39] R. Guidelli; R.G.Compton; J.M.Feliu; E.Gideali; J.Lipkowski; W.Schemickler and S.Trasatti. Difining the transfer coefficient in electrochemistry An assessment (IUPAC Tech. report). pure Appl. chem. 86(2): 245-258. 2014

[40] M. Shamsipur; M. Roushani; S. M. Pourmortazavi and N. Shahabadi. Amperometric determination of sulfide ion by glassy carbon electrode modified with multiwall carbon nanotubes and copper (II) phenanthroline complex. Cent. Eur. J. Chem. 12(10): 1091-1099. 2014